# Particulate and Trace Gas Emissions from Large Biomass Fires in North America

Lawrence F. Radke, Dean A. Hegg, Peter V. Hobbs,
J. David Nance, Jamie H. Lyons, Krista K. Laursen,
Raymond E. Weiss, Phillip J. Riggan, and Darold E. Ward

In this chapter we describe the results of airborne studies of smokes from 17 biomass fuel fires, including 14 prescribed fires and 3 wildfires, burned primarily in the temperate zone of North America between 34° and 49°N latitude. The prescribed fires were in forested lands and logging debris and varied in areas burned from 10 to 700 hectares (ha) (over a few hours). One of the wildfires ultimately consumed 20,000 ha and burned over a period of weeks. The larger fires produced towering columns of smoke and capping water clouds. As an indication of scale, the prescribed fires were visible only as small features in meteorological satellite imagery, but one of the wildfires studied produced a persistent, visible plume more than 1000 kilometers (km) long. Details of these fires and their fuels are given in Table 28.1.

The measurements were made aboard the University of Washington's C-131A research aircraft. This twin-engined, 20,000 kilogram (kg), propeller-driven airplane carries instrumentation for measuring the size and nature of aerosol particles, trace gas concentrations, and meteorological parameters. Major portions of the aerosol system have been described by Radke (1983) and the trace gas instrumentation has been described by Hegg et al. (1987). Details concerning the analysis of data, in addition to those presented in subsequent sections, can be found in Radke et al. (1988) and Hegg et al. (1990).

Our studies have focused on factors that could impact global climate through alteration of the earth's radiation balance. These include emissions of trace gases and smoke particles from biomass burning, the optical properties of the smoke, and the interaction of the smoke particles with water clouds.

## Particle Emission Factors

Particle (and other) emission factors for the fires were computed using the carbon-balance method of Ward et al. (1982) as adapted for aircraft sampling by Radke et al. (1988). This method requires in-plume measurements of all major carbon-containing products of combustion. These include $CO_2$ and CO, which are of primary importance, a less important subset of hydrocarbons ($CH_4$, $C_2H_2$, $C_2H_6$, $C_3H_6$, $C_3H_8$, and $C_4$ isomers), and the smoke particles (approximately 60% carbon). We assumed that all of the carbon in the fuel was released into the plume during the fire after being converted to the different carbonaceous products of combustion listed above. We further assumed that the concentration of particulate mass remained proportionally constant with reference to the concentrations of the gaseous products of combustion listed above for every Lagrangian parcel in the plume throughout the period of our measurements. This assumption is valid for particles with aerodynamic diameters less than 3.5 μm (a 3.5 μm cutpoint cyclone was used to remove larger particles before sampling on Teflon filters). The ratio of the mass concentration of carbon in the plume to the mass fraction of carbon in the fuel gives a measure of the mass of fuel required to produce the emissions contained in a unit volume of air in the plume after combustion. The reciprocal of this quantity, when multiplied by the corresponding concentration of particle mass, gives the particle emission factor (EF). This is summarized in the following equation:

$$EF = \frac{\overline{P}C_f}{(\overline{P}C_p) + (\overline{CO_2}C_{CO_2}) + (\overline{THC}C_{THC}) + (\overline{CO}C_{CO})} \quad (28.1)$$

where $\overline{P}$, $\overline{CO_2}$, $\overline{CO}$, and $\overline{THC}$ are the excess (i.e., above background) mass concentrations of aerosol particles, $CO_2$, CO, and total hydrocarbons, respectively; and $C_f$, $C_p$, $C_{CO_2}$, $C_{CO}$, and $C_{THC}$ are the fractional masses of carbon in the fuel, smoke particles, $CO_2$, CO, and total hydrocarbons, respectively. The derivation of equation (28.1) is given by Radke et al. (1988). For the current study we assumed a fuel carbon fraction ($C_f$) of 0.5 (Bryam, 1959; Susott et al., this volume, Chapter 32). $C_p$ is measured using programmed ramped temperature heating of quartz filters exposed to smoke, and analysis of the carbon

Levine, J.S. (ed), 1991. Global Biomass Burning: Atmospheric, Climatic, and Biospheric Implications. Cambridge, MA: MIT Press.

**Table 28.1** Fires examined in present study

| Fire | Date | Location | Size (ha) | Type of fire | Fuel |
|---|---|---|---|---|---|
| Abee | 22 Sept. 1986 | Montesano, Wash. | 40 | Prescribed | Debris from Douglas fir and hemlock |
| Eagle | 3 Dec. 1986 | Ramona, Calif. | 30 | Prescribed | Standing black sage, sumac, and chamise |
| Lodi 1 | 12 Dec. 1986 | Los Angeles, Calif. | 40 | Prescribed | Standing chaparral, chamise |
| Lodi 2 | 22 June 1987 | Los Angeles, Calif. | 150 | Prescribed | Standing chaparral, chamise |
| Hardiman | 28 Aug. 1987 | Chapleau, Ont. | 325 | Prescribed | Debris from jack pine, standing aspen, and paper birch |
| Wheat | 31 Aug. 1987 | Rosalia, Wash. | ~10 | Prescribed | Wheat stubble |
| Myrtle/Fall Creek | 2 Sept. 1987 | Roseburg, Ore. | 2,000 | Wildfire | Standing pine, brush, and Douglas fir |
| Silver | 17–19 Sept. 1987 | Grants Pass, Ore. | 20,000 | Wildfire | Douglas fir, true fir, and hemlock |
| Satsop | 19 Sept. 1987 | Satsop, Wash. | 40 | Prescribed | Debris from Douglas fir and hemlock |
| Troy | 8 Oct. 1987 | Troy, Mont. | 70 | Prescribed | Debris from pine, Douglas fir, and true fir |
| Battersby | 12 Aug. 1988 | Timmins, Ont. | 718 | Prescribed | Jack pine, white and black spruce |
| Peterlong | 22 Aug. 1988 | Timmins, Ont. | 217 | Prescribed | Jack pine, white and black spruce |
| Carbonado | 27 July 1989 | Enumclaw, Wash. | 40 | Prescribed | Debris from Douglas fir and hemlock |
| Summit | 1 Aug. 1989 | Grangeville, Idaho | 100 | Wildfire | Debris from pine, Douglas fir, and true fir |
| Hill | 10 Aug. 1989 | Chapleau, Ont. | 486 | Prescribed | "Chained" and herbicidal paper birch and poplar |
| Wicksteed | 12 Aug. 1989 | Hornepayne, Ont. | 700 | Prescribed | "Chained" and herbicidal birch, poplar, and mixed hardwoods |
| Mabel Lake | 25 Sept. 1989 | Kelowna, B.C. | 29 | Prescribed | Debris from hemlock, deciduous, Douglas fir |

released with the pyrolysis products (Johnson et al., 1981).

The derived emission factor is strictly valid only at the point of measurement. Any process that adds or removes a pollutant between the source and the location of the measurement will change the derived emission factor for that pollutant. Such changes are negligible if the measurements are made close to the fire, but at high altitudes or at long distances downwind, mechanisms such as cloud scavenging and gas-to-particle conversion may significantly change the measured values of the emission factors. The emission factors for particle mass given below were derived from measurements in smoke columns above the fire or at short distances downwind in stabilized smoke plumes. In some cases, however, the plume had been scavenged by capping cumulus clouds.

Many of the prescribed biomass fires studied exhibited marked temporal characteristics. Most of the fires began with intense combustion and long flame lengths as the small, dry fuels (leaves, needles, twigs, etc.) burned. Particle emission factors during this period were comparatively small and the smoke appeared rather dark (in some cases very dark) at visible wavelengths. Some of the smaller fires (those which ignited rapidly) then evolved naturally into a state characterized by combustion of the predominantly "smoldering" type. Compared with the initial "flaming" phase of combustion, the "smoldering" phase was marked by higher emission factors and light gray to white smokes. This type of progression was observed at the Mabel Lake fire (Figure 28.1), where the particle emission factor increased by a factor of almost three as the fraction of the total fire characterized by smoldering combustion increased (it took most of the first 18 minutes after ignition for the smoke to rise from the surface to the 3 km sampling altitude of the aircraft).

A similar temporal progression was observed at the Abee prescribed burn (Figure 28.2), except that the particle emission factor decreased again near the end of the fire. Here, the fuels were similar to those at Mabel Lake, the most notable difference being that the Abee fire was in the Pacific coastal region of Washington while the Mabel Lake fire was in the interior of British Columbia. In spite of the fuel similarities, the emission factors measured at the Abee fire were much greater than those measured at Mabel Lake. The Abee fire had the highest emission factors, for a sustained period, of any fire in this study. The emission factor increased rapidly over the first 25 minutes of combustion. However, during the initial 10 to 15 minutes the smoke column was capped by a vigorous cumulus cloud (about 1.5 km in depth) that may

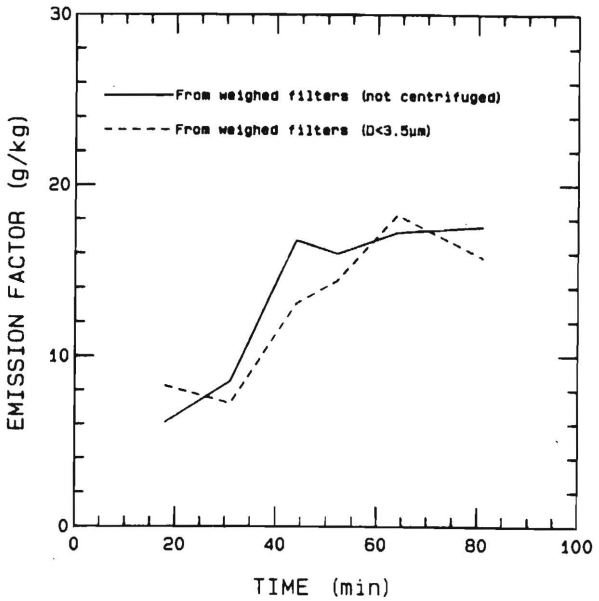


**Figure 28.1** Emission factors for particle mass as a function of time after ignition for the Mabel Lake fire.

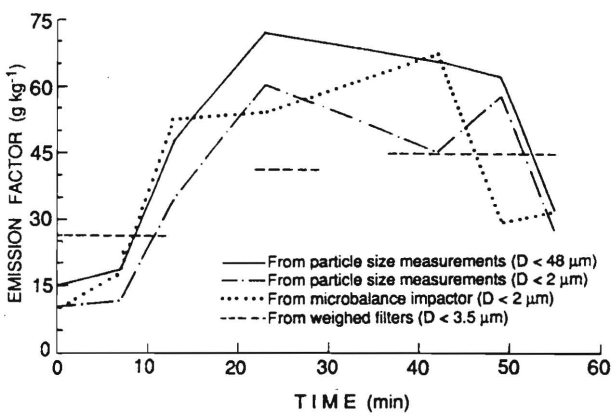


**Figure 28.2** Emission factors for particle mass as a function of time from the beginning of observations on the Abee fire. A vigorous cumulus cloud capped the smoke column for the first 10 to 15 min. The measurements were made downwind of this capping cumulus in the stabilized plume of smoke (from Radke et al., 1988).

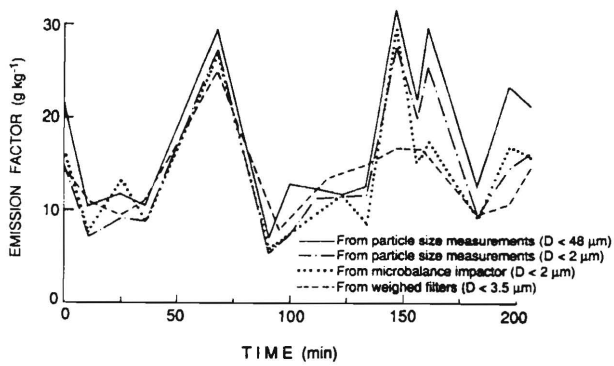


**Figure 28.3** Emission factors for particle mass as a function of time after ignition for the Lodi 1 fire (from Radke et al., 1988).

have significantly scavenged the smokes (we have no quantitative estimates of scavenging by this cloud; however, as we will discuss in a later section, we observed no significant scavenging of accumulation mode smoke particles by any other cumulus cloud with a vertical depth less than 2 kilometers. Thus, we interpret this period of relatively low emission factors as being caused by some combination of efficient, predominantly flaming combustion and cloud scavenging.

Other temporal responses of this type were observed in an earlier study of smaller (<5 hectares) fires in Oregon (Radke et al., 1990) and by Ward and Hardy (in press) in their study of 38 prescribed test fires where the products of combustion (CO, $CO_2$, $CH_4$, nonmethane hydrocarbons, and particles less than 2.5 μm) were found to produce a continuum of data as a function of combustion efficiency. They define combustion efficiency as the percent of the carbon contained in the fuel that is completely oxidized to $CO_2$ during combustion. Combustion efficiency was found to be 90% to 95% for the flaming phase and 60% to 90% for the smoldering combustion phase in their study.

Most of the remaining fires listed in Table 28.1, particularly the larger ones, were characterized by multiple periods of ignition that produced complex temporal patterns. Lodi 1 (Figure 28.3) was such a fire.

Average particle emission factors for each of the fires are listed in Table 28.2. The three sets of values shown represent results derived from volume integrated size distributions for particles with diameters <2 μm and an assumed particle density, from smoke particle masses on weighed filters that were preceded by a centrifuge with an aerodynamic particle cut <3.5

**Table 28.2** Particle emission factors (in grams of smoke per kilogram of biomass fuel burned) and single-scattering albedo and specific absorption for all fires studied

| | Emission factor (derived from size distribution of particles) (<2 μm diameter) | | | Emission factor (from weighted filters containing particles) (<3.5 μm diameter) | | | Emission factor (derived from size distribution of particles) (<48 μm diameter) | | | | |
|---|---|---|---|---|---|---|---|---|---|---|---|
| | Mean | Standard deviation | Number of samples (N) | Mean | Standard deviation | Number of samples (N) | Mean | Standard deviation | Number of samples (N) | Mean value of single-scattering albedo ($\tilde{\omega} = \sigma_s/\sigma_E$) | Mean values of specific absorption $B_A$ ($m^2\ g^{-1}$) |
| Abee | 35.1 | 20.3 | 7 | 37.4 | 9.8 | 3 | 44.5 | 23.1 | 7 | ND | ND |
| Eagle | 7.9 | 5.7 | 8 | 11.3 | 4.8 | 2 | 10.8 | 6.0 | 8 | 0.85 (N = 2) | 0.67 (N = 2) |
| Lodi 1 | 14.3 | 7.3 | 16 | 13.5 | 4.4 | 13 | 17.6 | 7.9 | 16 | 0.89 (N = 13) | 0.74 (N = 13) |
| Lodi 2 | 15.5 | 6.5 | 9 | 23.0 | 19.6 | 8 | 17.7 | 7.0 | 9 | 0.80 (N = 7) | 0.68 (N = 1) |
| Hardiman | 16.2 | 12.4 | 11 | 10.5 | 3.0 | 9 | 21.7 | 14.6 | 11 | 0.87 (N = 9) | 0.79 (N = 5) |
| Wheat | 43.8 | — | 1 | ND | — | — | 47.9 | — | 1 | NA | ND |
| Myrtle/FallCreek[a] | 19.5 | 12.1 | 10 | 6.1 | 3.1 | 8 | 29.3 | 16.5 | 10 | 0.84 (N = 4) | 0.73 (N = 16) |
| Silver[a] | 26.4 | 13.6 | 2 | 20.2 | 12.7 | 3 | 32.5 | 17.1 | 2 | 0.90 (N = 2) | 0.36 (N = 2) |
| Satsop | 24.6 | 7.1 | 2 | 12.0 | — | 1 | 34.3 | 10.8 | 2 | 0.86 (N = 1) | 0.38 (N = 1) |
| Troy | 17.1 | 12.4 | 5 | 9.7 | 3.0 | 5 | 30.2 | 19.5 | 5 | 0.82 (N = 3) | 0.82 (N = 3) |
| Battersby | 18.2 | 21.1 | 11 | 20.9 | 10.6 | 11 | 20.3 | 20.7 | 11 | 0.84 (N = 7) | 0.89 (N = 4) |
| Peterlong | ND | ND | ND | 16.9 | 5.1 | 4 | ND | ND | ND | 0.84 (N = 4) | 1.39 (N = 2) |
| Hill | 5.5 | 3.5 | 6 | 10.2 | 6.5 | 3 | 6.9 | 4.3 | 6 | 0.84 (N = 3) | 0.59 (N = 4) |
| Wicksteed | 12.9 | 9.1 | 10 | 10.8 | 4.7 | 5 | 13.3 | 9.1 | 10 | 0.60 (N = 6) | 0.66 (N = 5) |
| Carbonado | 10.7 | 7.6 | 7 | ND | — | — | 11.1 | 7.9 | 7 | 0.89 (N = 9) | ND |
| Summit[a] | 17.6 | 4.1 | 2 | ND | — | — | 18.33 | 4.4 | 2 | 0.82 (N = 5) | ND |
| Mabel Lake | 19.9 | 8.4 | 5 | 12.8 | 4.3 | 6 | 23.4 | 5.9 | 3 | 0.82 (N = 12) | 0.41 (N = 14) |
| Averages | 16.4 | 13.2 | 112 | 15.0 | 10.6 | 81 | 21.2 | 15.4 | 110 | 0.83 ± 0.11 (N = 83) | 0.64 ± 0.36 (N = 73) |

a. Wildfires.
NA = not analyzed.
ND = no data.

μm, and from volume integrated size distributions for particles with diameters <48 μm. The weighed filter approach is the simplest and most accurate.

As shown in Table 28.2, the emission factor for biomass smoke particles with aerodynamic diameters <3.5 μm averaged 15.0 grams per kilogram of fuel burned. Particles of this size contribute overwhelmingly to the light-scattering coefficient and visual light produced by smokes. They also have atmospheric residence times of a few days to weeks depending on the altitude to which they are lofted and whether they are scavenged by a capping cumulus cloud. During the flaming phase of combustion, a high rate of heat release can generate a very strong central convection column capable of lofting smoke particles to high altitudes (>6 km). However, lifting of this magnitude also has the potential to produce large cumulus clouds that are capable of scavenging substantial portions of the lofted smoke (see the section on cloud and precipitation scavenging of smokes). The net effect is still uncertain and needs further study.

Coarse and giant particles, which have diameters between 2.0 and 48 μm, averaged about 20% of the particulate mass. Electron microscopy showed these particles to be a mixture of coagulation products and fuel and soil debris.

It is presumed that much of the variance in the particle emission factors that we measured is due to the changing proportional contributions from different phases of combustion typical of biomass fires, although this is difficult to quantify from an airborne perspective. Because of this difficulty, it is not clear how much of the total variance remains unexplained. However, additional factors influencing particle emissions have been uncovered.

Stith et al. (1981) noted an increase in emissions with increasing fuel moisture. Cofer et al. (1989), Ward (1989), and Hegg et al. (1990) suggest that combustion efficiency in open fires also depends on the amount of oxygen delivered to the combustion zone by turbulent airflows. Thus, some fires, especially large ones, may be characterized by periods of oxygen depletion or perhaps by "thermal quenching" of oxidation reactions. In many of the fires studied the particle emission factor increased as the supply of oxygen to the combustion zone decreased. An example is the Battersby fire (Figure 28.4). Here we use the ratio of CO to $CO_2$, which gives a measure of the extent of oxidation in the plume, as an indicator of oxygen availability, with high ratios suggesting limited oxygen (further discussion of this phenomenon is presented in the section on trace gas emissions).

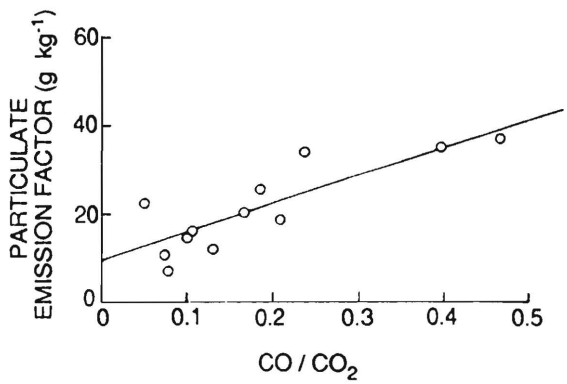


**Figure 28.4** Emission factors for particles as a function of the $CO/CO_2$ concentration ratio in the plume from the Battersby fire. The $CO/CO_2$ ratio is a measure of the extent of oxidation in the plume, with higher values indicating less oxidation (from Hegg et al., 1990).

In view of the difficulty of accounting for all of the variability in particle emissions from biomass fires, our studies may not have bounded the full range of emission factors possible from open fires of biomass fuels. Fires with greater areal extent than those studied here could have significantly larger smoke particle emission factors. It should also be noted that the prescribed fires studied here occurred within a restricted set of meteorological and fuel moisture conditions designed to prevent fire escape yet still allow an acceptable fraction of the fuel to burn. Extreme conditions that give rise to rapidly moving wildfires may produce different smoke emission factors.

### Particle Size Distributions

The size distributions of particles in the smokes displayed a high degree of consistency. The particle volume distributions in particular showed comparatively little variation in shape from one fire to another or during any one fire while near the source, although particle concentrations varied widely. Shown in Figure 28.5 are average number and volume distributions measured in the smoke plumes at distances about or <5 km from three fires. These size distributions are much like those of other urban/industrial pollution aerosol, with three distinguishable modes: a nucleation mode (diameters <0.1 μm), an accumulation mode (diameters from 0.1 to 2.0 μm), and a coarse mode (diameters >2.0 μm). For reasons probably related to different particle generation mecha-

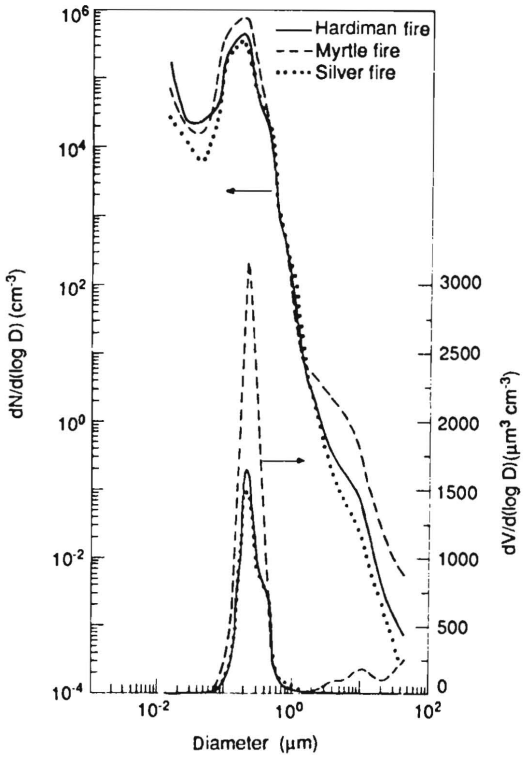


**Figure 28.5** Average number and volume distributions of particles measured in the smoke plumes near (<5 km from) the sources of three fires (from Radke et al., 1988).

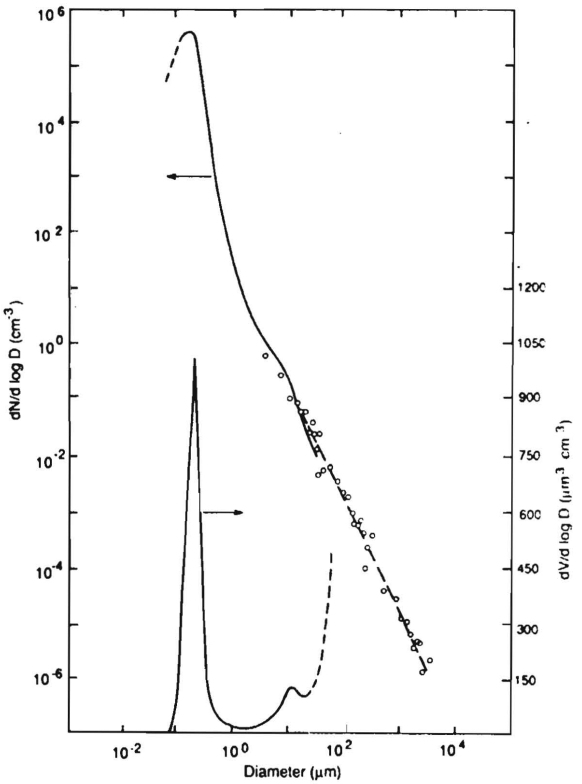


**Figure 28.6** Mean number and volume distributions of particles measured in the ascending column at the Lodi 1 fire. Data points representing large, giant, and supergiant particles were measured with laser hydrometer cameras.

nisms for the accumulation and coarse mode aerosol, there is a pronounced minimum in the particle volume distributions in the region between 1.0 and 3.0 μm diameter that separates these two modes. Not only was this characteristic of the smoke from these fires, but it also seems to be generally true in the atmosphere. The accumulation mode often dominated both the number and volume distributions. Particles in the accumulation mode consisted primarily of tarry, condensed hydrocarbons that were typically spherical in shape. The fraction of accumulation mode particles that were nonspherical aggregates was rather small, especially when compared to smokes from fossil fuel fires (Radke et al., 1990b). The biomass smoke particles also contained some water-soluble inorganics (primarily $SO_4^=$ and $NO_3^-$; Hegg et al., 1987), which accounts, in part, for their activity as very efficient cloud condensation nuclei (Radke et al., 1978; Hallet et al., 1989).

The magnitude of the coarse particle mode showed considerable variation. For example, in the Lodi 1 fire (chaparral fuel type), there was a mode near 10 μm comprised mostly of condensed hydrocarbons aggregated with a significant fraction of soil particles (Cofer et al., 1988). In addition to this mode, an examination of the data from our laser hydrometer cameras showed that particles of ash and soil debris up to and exceeding 1 millimeter (mm) in diameter were often present in concentrations greater than 10 $m^{-3}$ (Figure 28.6). Although there were large variations in the concentrations of these supergiant particles, their presence was typical of all the large fires studied. Lofting of soil and ash at Lodi 1 has also been reported by Einfeld et al. (1989). The amount of coarse mode particles from fires of biomass fuels may be related to the rate of heat release and to horizontal and vertical wind velocities (Ward, 1990; Susott et al., this volume). On occasion, the mass in the coarse mode exceeded that in the accumulation mode. It is important to remember that coarse mode and especially supergiant particles are generally undercounted and, despite our efforts to improve the sampling efficiencies of these particles, were probably underestimated here as well.

The nucleation mode was the most variable mode in these smokes. It was occasionally the most promi-

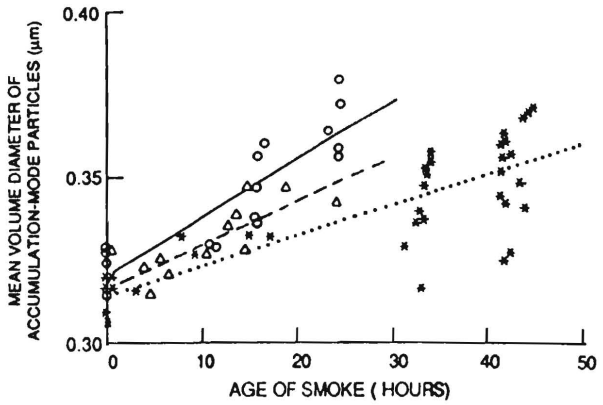


**Figure 28.7** Geometric mean volume diameter of particles in the accumulation mode (0.2 to 2 μm diameter) as a function of the age of the smoke in the plume of the Silver fire. The measurements are grouped according to the value of the light-scattering coefficient due to dry particles as follows: stars and dotted lines: $2 \times 10^{-4}\ m^{-1} < \sigma_{sp} < 5 \times 10^{-4}\ m^{-1}$ ($r = 0.89$); triangles and dashed lines: $5 \times 10^{-4}\ m^{-1} < \sigma_{sp} < 5 \times 10^{-3}\ m^{-1}$ ($r = 0.77$); circles and solid lines: $\sigma_{sp} > 5 \times 10^{-3}\ m^{-1}$ ($r = 0.81$).

nent mode in the number distribution, but more often it was much smaller than the accumulation mode, and it seldom contained significant particle mass. Its mode concentration is largely driven down by coagulation very near the fire (Fuchs, 1964) and up by continuing gas-to-particle conversion in the smoke plumes.

Coagulation also affects the mean size of the accumulation mode, although particle concentrations need to be rather large for a long period of time to obtain definitive measurements. The dependence of the coagulation rate on particle concentration is illustrated in Figure 28.7, where the smoke from a large multi-wildfire conflagration (Silver) was tracked for more than 1000 km (about 48 hours downwind from the source). The geometric mean volume diameter of the particles in the accumulation mode generally increased with age for all samples. The rate of increase was positively correlated with the light-scattering coefficient due to dry particles ($\sigma_s$), which is generally proportional to the mass concentration of particles in the accumulation mode (Waggoner et al., 1981). This result is to be expected for a process dominated by coagulation.

Intermode coagulation is also evident in the Silver fire data. Samples taken at various distances downwind of the fire showed a general decline with age in the volume concentrations of particles in the nucleation and accumulation modes, while the volume concentrations of particles in the coarse-particle mode increased with age. This was, presumably in large part, due to coagulation, which is a sink for smaller particles and a source for larger particles, with mass being added to the small size end of the coarse mode faster than sedimentation can remove particles from the larger end. These smoke samples were normalized by the CO concentration (which we assumed was conserved in the plume) to compensate for the dilution effects of plume dispersion (for details, see Radke et al., 1990a).

## Optical Properties

The optical properties of smoke particles are often described by the volume optical extinction coefficients ($\sigma_e$, $\sigma_s$ and $\sigma_a$, where the subscripts indicate the form of extinction—*e* for total extinction, *s* for scattering, and *a* for absorption), the specific or mass normalized extinction ($B_i = \sigma_i/\rho$, where $\rho$ is the mass concentration and *i* again represents the form of the extinction coefficient), and the albedo for single scattering ($\tilde{\omega} = \sigma_s/\sigma_e$). The extinction coefficients depend on the complex refractive index of the particles, their size distribution and concentration. The specific extinction and the albedo for single scattering are normalized to concentration and therefore depend only on the fundamental chemical and physical properties of the particles.

Direct, in-situ measurements of $\sigma_e$ and $\sigma_s$ over a range of wavelengths centered on 540 nm yielded $\sigma_a$ by the relation $\sigma_a = \sigma_e - \sigma_s$ (Weiss and Radke, 1990). This permitted real-time measurements with a time resolution of about 1 second (about 80 meters of flight path). $\sigma_e$ is measured with an optical extinction cell (OEC). The OEC is an enclosed, 6.4 meter path length photometer designed to measure the change in brightness of a regulated light source over a single pass of the cell. For smoke plume studies, an initial brightness measurement ($I_o$) was taken of background air prior to entering the plume and this was compared continuously to brightness of the light source ($I$) with plume air flowing through the cell. A reference light path was used to normalize all light measurements to constant lamp brightness. $\sigma_e$ was calculated continuously from

$$\sigma_e = (1/L)\ln[I_o/I] \qquad (28.2)$$

where $L$ is the length of the cell. In the aircraft, sample flow was supplied by ram air through a nearly isokinetic probe protruding ahead of the aircraft through the forward cabin wall. Near the entrance to

the OEC, the sample flow was split to provide parallel flow to the nephelometer and the OEC.

Preflight calibration of the OEC/nephelometer system was accomplished by ensuring that $\tilde{\omega}$ did not deviate from unity for laboratory generated nonabsorbing particles (such as polyethylene glycol, NaCl, or $(NH_4)_2SO_4$) with an appropriate and known size distribution. This system has been used by us since December 1986 beginning with the Lodi 1 prescribed burn near Los Angeles.

The optical properties of smoke particles from biomass burning can be highly variable. They appear to depend on a number of factors, including the type of fuel burned, the intensity of the fire, flame height, and the phase of combustion (McMahon, 1983; Patterson and McMahon, 1984). In the early, flaming phase of combustion, when both high temperatures and oxygen deprivation prevail, conditions support pyrolytic production of particles consisting of high concentrations of both single spheres and sooty chains that are optically very absorbing. In the later, smoldering phase of combustion, smoke production is dominated by weakly or nonabsorbing liquid (waxy) and solid particles, consisting of organic materials with a range of volatility, and nonsooty inorganic materials.

Patterson and McMahon (1984) measured specific absorption of smoke particles collected on filters exposed to laboratory fires of pine needles. They found a substantial increase in the production of elemental (or sooty) carbon in the flaming phase of combustion relative to the smoldering phase, with the specific absorption coefficient ranging from 0.04 $m^2\ g^{-1}$ for the smoldering phase to 1.0 $m^2\ g^{-1}$ for the flaming phase. These were measurements on smokes in a laboratory environment where burning conditions were controlled. In larger fires of over 100 ha the smokes often consist of mixtures of particles from all combustion stages. However, we studied two prescribed fires where the transition from a mostly flaming phase to the smoldering phase was evident in the optical properties.

The two fires were the Troy fire (8 October 1987) and the Mabel Lake fire (25 September 1989). Both were small fires (70 and 29 ha, respectively) of downed debris consisting of mixed wood types in which there was intense burning in the initial stages of combustion and relatively uncomplicated meteorological conditions. In both fires the aerosol was optically dark during the early stages of intense burning and became less dark as the fires progressed to a predominantly smoldering phase. This result is shown in Figure 28.8, where it can be seen that the single-scattering albedo (measured at altitudes of 2 to 2.5 km) was initially less than 0.7 in both fires and approached a relatively stable value of about 0.9 during the smoldering phase. Mean values of specific absorption for both fires were approximately 0.4 $m^2g^{-1}$, which is similar to the laboratory average values reported by Patterson and McMahon (1984).

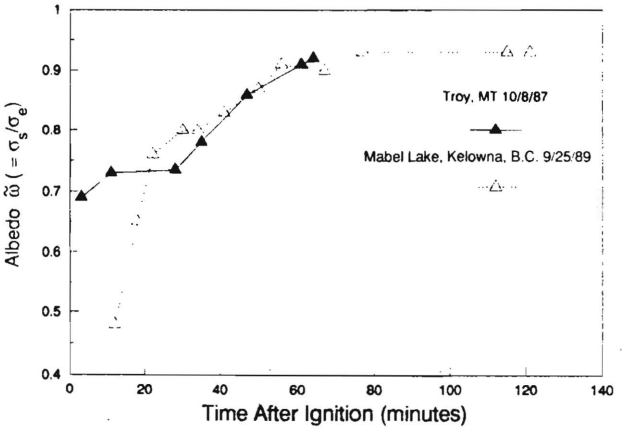


**Figure 28.8** The time evolution of the single-scattering albedo $\tilde{\omega}$ for smoke from the Troy (solid triangles) and Mabel Lake (hollow triangles) prescribed burns.

Mean values of $\tilde{\omega}$ and $B_a$ for each of the 17 biomass fires in this study are listed in Table 28.2. The average albedo was 0.83 ± 0.11 and the specific absorption was 0.64 ± 0.36 $m^2\ g^{-1}$, indicating that biomass smokes are typically grey-white in visual appearance.

All of these fires produced periods (usually less than 10% of the fire's temporal extent) of dark smokes. One of the largest prescribed fires in the program (Wicksteed) produced the darkest plume cross-section (average albedo = 0.37). Since there is reason to believe that exceptionally large fires might be characterized by oxygen deficient flaming combustion, with large particle emission factors and low albedos, this result suggests that it would be desirable to take measurements in the smokes from fires larger than the largest in this study, or in a "blow up" or mass wildfire.

Finally, the visible wavelength albedo of biomass smokes appears to be modified by interactions with clouds. Smokes that pass through a cumulus cloud typically experience an increase in albedo of as much as 10% (smokes become whiter). Although the exact mechanism for increased albedo from cloud detraining smoke is not known, gas-to-particle conversion, chain aggregate collapse, coagulation, dilution and albedo-dependent scavenging may all play a role.

## Biomass Smokes as a Source of Cloud Condensation Nuclei

Warner and Twomey (1967) and Hobbs and Radke (1969) noted (with some surprise) that agricultural and forestry biomass burning produced copious quantities of rather efficient cloud condensation nuclei (CCN). Further, it was found that these particles affected cloud droplet concentrations and size distributions, even for cumulus clouds with "continental" droplet concentrations. See, for example, the observations of Eagan et al. (1974) downwind of a small wildfire in coniferous forest lands in Washington state. Such measurements indicate the power of biomass combustion CCN to have a major impact on cloud microphysics (for further discussion see Radke, 1989).

Recent attempts to quantify the amounts of biomass burned globally (NAS, 1984, 1986) together with more quantitative work on smoke particle size, smoke mass yield per mass of biomass burned, and the ratio of CCN to total smoke particles (Radke et al., 1988; Hallett et al., 1989) encourage an estimate of the global CCN production from this source. Such estimates are important to the global change issue since global burning is far more extensive in the tropics and the production of CCN by industrial pollution may be less prominent.

There are a number of ways to estimate the CCN source strength, but, in keeping with the measurement uncertainties, a simple approach seems justified. If it is assumed that about $5 \times 10^{12}$ CCN are produced for every gram of biomass burned (Warner and Twomey, 1967), and that about $7 \times 10^{12}$ kg of biomass are burned every year (Seiler and Crutzen, 1980), then an annual average estimated global production of about $3.5 \times 10^{28}$ CCN per year or about $10^{21}$ CCN $s^{-1}$ from biomass burning is the result. An alternative estimate is obtained by observing that about 30%–100% of submicron biomass smoke particles serve as CCN (Hallett et al. 1989), that such submicron smoke is produced with an efficiency of about 15 g $kg^{-1}$ of biomass burned (from Table 28.2), and that the particle mass median diameter of such smoke is about 0.3 μm (from Figure 28.5). Assuming that the density of a 0.3 μm diameter smoke particle averages 1.0 g $cm^{-3}$ (Stith et al., 1981; Radke et al., 1990), one finds a production rate of about $1–3 \times 10^{20}$ CCN $s^{-1}$. The uncertainties in both of these calculations are at least an order of magnitude. Thus, the result of this simple analysis is that the direct emission of particles from global biomass burning produces about $10^{19}–10^{22}$CCN $s^{-1}$. This rate is similar to estimates of global CCN production from oceanic (Radke, 1989; Twomey and Wojciechowski, 1969) and industrial (Radke and Hobbs, 1976) sources of CCN. CCN production must have a seasonally magnified impact, especially in the tropics because of the dominance of biomass burning as a source of CCN and the seasonal nature of biomass consumption by fires. The same may apply to CCN production from biomass fires in the boreal and temperate regions. Here, however, the anthropogenic sources for CCN would be comparable to that from biomass fires.

## Cloud and Precipitation Scavenging of Smokes

In the present sequence of experiments we have examined 17 biomass fires or fire complexes. Of these, 10 (Abee, Battersby, Carbonado, Hardiman, Hill, Myrtle/Fall Creek, Satsop, Troy, and Wicksteed) featured fire capping cumulus clouds and four (Hardiman, Battersby, Hill, and Wicksteed) reached cumulonimbus proportions. Of these four, the Hardiman fire produced only light to moderate precipitation and none may have reached the ground. At the other end of the intensity scale, the Hill fire produced a persistent, mature thunderstorm with heavy precipitation.

Our studies show that large fires can produce capping cumulus clouds that can substantially reduce total smoke emissions and that, contrary to the suggestion of Cotton (1985), biomass smokes are not resistant to prompt and efficient cloud and precipitation scavenging. Indeed, interactions with and removal by cloud processes appear to largely determine the residence time of smoke particles in the atmosphere since, for the accumulation mode at least, sedimentation and other forms of dry deposition are slow (Jaenicke, 1981).

Our approach to measuring scavenging efficiencies depends on a variety of sampling schemes, all of which face some difficulties for a single aircraft experiment. The choice of which approach to use is largely dependent on the size of the fire. The schemes that we have used are listed below, together with a brief critique of each:

1. *Aerosol deficit.* In principle, this is the simplest and most powerful approach. It requires measurements of an aerosol property (mass, size distribution, etc.) along with a conservative tracer believed to be proportional to the aerosol emitted (and largely insoluble in cloud water, e.g., CO) in the ascending smoke

column below cloud base and in the smoke exiting the capping cumulus cloud. The conservative tracer is used to correct smoke concentrations for dilution due to mixing with ambient air inside the cloud. The difficulty is that this method requires a period of steady-state emission.

2. *Emission factor.* We initially believed (based on ground observations) that the evolution of the particulate emission factor would be relatively slow as the phase of the fire moved from flaming to smoldering. Thus, a combination of emission factors measured below cloud base, interstitially (between cloud droplets) in the cloud, and exiting the cloud, would provide a useful measure of scavenging. Again, this requires a steady-state fire (which is uncommon); however, unlike the "aerosol deficit" method, a dilution correction is not required.

3. *Interstitial.* This requires measuring the ratio of the mass of smoke (or a surrogate for the smoke) interstitial to the cloud droplets and in the cloud droplets. After converting the amount in the cloud droplets to an equivalent air concentration (see Hegg et al., 1984), the ratio produces directly the scavenging fraction for the accumulation mode aerosol. If a surrogate for smoke is used (we used the sulfate accumulation mode aerosol coemitted integrally with the smoke), one must be satisfied that smoke is scavenged similarly, and that the surrogate is inert (i.e., it has no sources or sinks different or in addition to those for smoke).

4. *Cloud water.* This requires measuring in close time proximity the concentration of smoke particles going into the cloud and the amount of smoke in the cloud water. Using volumetric and cloud liquid water content measurements to yield equivalent air concentrations, the amount of accumulation mode aerosol scavenged is determined. This method suffers from the same problems as 3 above. In addition, errors will be introduced if the cloud is precipitating.

Our initial efforts focused on the "aerosol deficit" and the "emission factor" methods. Of these, only our work with "aerosol deficit" remains active since the "emission factor" method did not provide consistent results. The "aerosol deficit" method is most valid for small cumulus clouds (cloud depths <2 km), because the short time needed to sample just below cloud base and climb to measure the smoke escaping the cloud allows the period of required steady-state smoke emissions to be rather short.

Of the small cumulus cases examined, especially the cumulus capped wildfires (Myrtle/Fall Creek) and the Troy prescribed burn, no significant scavenging of accumulation mode particles occurred. Significant removal of the supermicron aerosol was observed. For the large cumulus, the Battersby fire produced clear results by the "aerosol deficit" method. The aerosol property examined was the particle size distribution. Shown in Figure 28.9 are the percentage removal of smoke particles as a function of particle diameter for two sets of measurements. Here we see most of the supermicron aerosol removed (95% to 100% in one case), a removal minimum at about 0.35 μm in particle diameter, and increased removal in the center of the smoke accumulation mode mass peak near 0.2 μm. Using the same method, the Hardiman fire produced similar results, with about 80% supermicron removal, about 40% accumulation mode removal, and a removal minimum at about 0.3 μm diameter (Figure 28.10). These results are for scavenging by all mechanisms. The vertical dashed line in Figures 28.9 and 28.10 represents our theoretically predicted mimimum particle size for nucleation scavenging, which was computed using the cloud droplet size distribution measured just above cloud base. Interestingly, the result of this calculation falls in the region of minimum scavenging efficiency. The mechanism responsible for the efficient removal from 0.1 to about 0.3 μm is uncertain. However, it is clear that significant smoke scavenging occurs with the onset of only

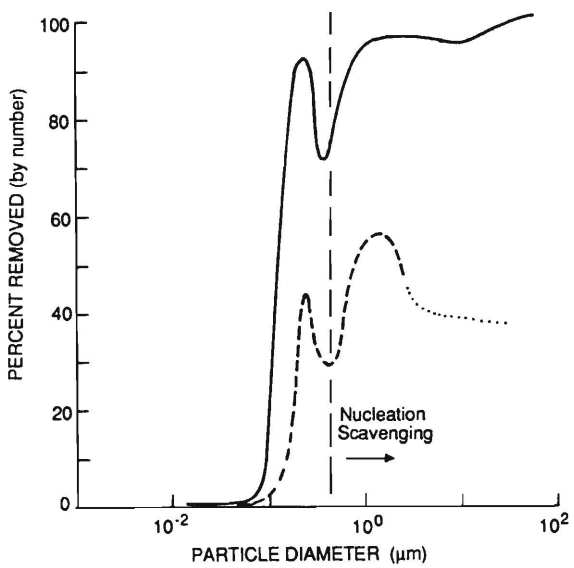


**Figure 28.9** Two measurements of the percentage of the mass of smoke removed by cloud and precipitation scavenging as a function of smoke particle size for the Battersby biomass fire. The vertical line marks the calculated lower size limit of a nucleation scavenging mechanism.

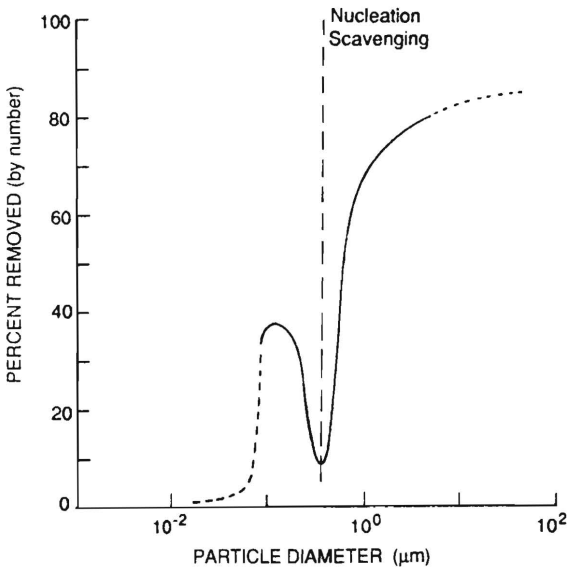


**Figure 28.10** As for Figure 28.9 but for the Hardiman biomass fire.

**Table 28.3** Mass scavenging efficiencies by cloud and precipitation processes for submicron diameter smoke particles

| Fire | Method 3 ("interstitial") | Method 4 ("cloud water") |
|---|---|---|
| Hill | — | 50 ± 30%<br>40 ± 20% |
| Wicksteed | 75 ± 20% | 80 ± 50% |

Note: See text for description of these two methods.

slight precipitation and it appears to increase with precipitation intensity.

The large Hill and Wicksteed biomass fires, which produced considerable precipitation, allowed scavenging estimates by the "interstitial" and "cloud water" methods; the results are summarized in Table 28.3. The Hill fire, which provided good data for a calculation by the "cloud water" method, yielded scavenging efficiencies of 40% to 50% for accumulation mode particles. The same method applied to the Wicksteed fire showed about 80% removal. Additional measurements obtained at Wicksteed allowed the use of the "interstitial" method, which produced a nearly identical scavenging efficiency of 75% for accumulation mode particles.

The difference between the scavenging efficiencies computed for the Hill and Wicksteed fires may be related to the concentration of smoke particles within the smoke plumes. The rate of release of smoke particles at the Hill fire was approximately three times greater than that for the Wicksteed fire during the times when measurements were taken. If the accumulation mode particles were being mostly cloud nucleation scavenged, the theoretical studies of Jensen and Charlson (1984) suggest that some scavenging limits could be reached that are inversely proportional to the concentrations of the inputted aerosol. This is in accord with our observations. However, since it is not clear that nucleation scavenging was the primary route by which the accumulation mode smoke entered the liquid water phase (in fact, the Battersby data suggests that it is not), speculations on the issue are premature.

The four large Canadian prescribed fires that produced cumulus clouds have provided us with significant new experimental evidence suggesting that scavenging of biomass smokes by capping cumulus clouds can be quite efficient. The cloud scavenging picture which emerges is:

- Supermicron smoke particles are removed with considerable efficiency in all but the smallest capping cumulus clouds. These particles no doubt participate in the early production of precipitation-sized drops.
- Accumulation mode smoke particles (which represent the bulk of the smoke particles with potentially great atmospheric residence times) can enter cloud water with significant efficiency (40% to 80%) and are removed from the cloud with equal efficiency (30% to 90%) by precipitating cumulus with depths greater than 2 km.

## Trace Gas Emissions

Emissions of trace gases from biomass burning are known to be an important source of several trace gases (such as $CO_2$, CO, and $CH_4$) in the atmosphere (Crutzen et al. 1985). In addition, local and regional air quality can be greatly affected by the emissions from fires (Radke et al., 1978). Nevertheless, quantitative assessments of the contributions of these emissions to the global budgets of certain trace gases are difficult to make. Biomass burning worldwide is not well quantified, either as to the area burned or to the proportion of the total mass of biomass consumed for a given area. In addition, emissions of trace gases are dependent on the fuel's chemical and physical properties. (Work is in progress at the Intermountain Fire Sciences Laboratory of the U.S. Forest Service to develop models that can be used for predicting the release of trace gases from biomass fires in fuels ex-

hibiting different chemical and physical properties) (Ward, 1990). Despite these shortcomings, the emissions from various temperate zone biomass fires show considerable consistency.

The trace gas data gathered in our measurements on the smokes from biomass burning not only warrants attention in its own right but encourages its use for extrapolation to global scales. The contributions of emissions from fires to global trace gas fluxes can be most simply calculated using available estimates of the amounts of CO and $CO_2$ produced annually from biomass burning (e.g., Crutzen et al., 1985; Mooney et al., 1987). To make use of this information, the relative emission ratio of each of the trace gases we measured to CO (or $CO_2$) was calculated using the data listed in Table 28.4. This value was then multiplied by the estimated worldwide emission flux of CO (or $CO_2$) from biomass burning, to yield an estimate of the contribution of biomass fires to the global flux of each trace gas measured. Since our estimates for $CO_2$ emissions (see Table 28.4) are, in general, somewhat higher than published values, CO has been used as the "ratio species" in our estimations of global fluxes.

Table 28.5 lists the mean emission factor ratios for certain trace gas species, as well as the estimated fluxes from global biomass burning found using these ratios. The value for worldwide CO emissions due to biomass burning used in calculating the fluxes was 800 teragrams per year (Tg $yr^{-1}$) (Crutzen et al., 1985). By way of comparison, a calculation using Radke's (1989) estimate of about $10^4$ Tg $yr^{-1}$ of biomass burned globally and our emission factor for CO, yields an essentially identical global flux of 910 Tg $yr^{-1}$ of CO.

Ozone, the first species listed in Table 28.5, is not emitted directly during combustion of biomass but is instead the product of the chemical interaction of reactive hydrocarbons and $NO_x$ in the smoke plume (Evans et al., 1974; Radke et al., 1978). The correlation between available $NO_x$ and the production of $O_3$ can be examined by studying the relationship between our emission factors for $O_3$ and $NO_x$. A linear regression of the $O_3$ emission factor onto the $NO_x$ emission factor (based on the data in Table 28.5) results in an intercept of $-2.2$ Tg $yr^{-1}$, a slope of 1.4, and a correlation coefficient ($r$) of 0.8 significant at the 98% confidence level. This suggests that $O_3$ is produced in smoke plumes in a process similar to that involved in photochemical smog production. As has been discussed previously (see Dismitriodes and Dodge, 1983), the mechanism responsible for $O_3$ production is apparently regulated by the availability of $NO_x$. If the amount of $NO_x$ in the plume is insufficient to react with the available reactive hydrocarbons, $O_3$ will not be produced. Correspondingly, the production of $O_3$ increases with increasing $NO_x$.

The contribution of emissions from biomass burning to global ozone fluxes can also be assessed using our results. Total tropospheric $O_3$ production has been estimated to be on the order of about 4,000 Tg $yr^{-1}$ (Hegg et al., 1990). This is two orders of magnitude greater than the value for the global flux of $O_3$ listed in Table 28.5 (32 Tg $yr^{-1}$). Consequently, biomass burning is a minor source of tropospheric ozone.

Based on our data, the estimated flux of $NH_3$ from global biomass burning is on the order of about 8 Tg $yr^{-1}$. This value represents roughly 50% of the total worldwide flux of the species, thereby substantiating a previous assertion (see Hegg et al., 1988) that emissions from biomass burning are a significant source of atmospheric $NH_3$.

A study of biomass fires in the Amazon Basin by Andreae et al (1988) yielded measurements of significant fluxes of particulate $NH_4^+$. The authors postulated that if these emissions also contained large amounts of gaseous $NH_3$ (which they did not measure), the contribution of biomass burning to the global flux of $NH_3$ would be quite substantial. Our global flux estimate for $NH_3$ of 8 Tg $yr^{-1}$ is approximately twice the flux of $NH_4^+$ from biomass fires (as estimated by Andreae et al.). If the fluxes of $NH_4^+$ and $NH_3$ are assumed to be additive, one obtains a combined flux of about 10 Tg $yr^{-1}$. This flux would then be the most significant contributor to the atmospheric $NH_3$ reservoir (see Galbally, 1985).

The estimated worldwide flux of $CH_4$ listed in Table 28.5 (32 Tg $yr^{-1}$) agrees favorably with previously calculated values (for example, Crutzen et al., 1985, obtained a global flux of 40 Tg $CH_4$ $yr^{-1}$). Furthermore, measurements of $CH_4$ emissions from the 10 fires illustrate an important characteristic of biomass fires. As is discussed by Hegg et al. (1990), the ratio of CO to $CO_2$ in a smoke plume serves as an indicator of the extent of oxidation in a plume, with high ratios indicating only limited oxygen availability. In such an oxygen-limited environment, the amount of $CH_4$ produced would be expected to be higher due to greatly increased $H_2$ levels (the relationships between concentrations of $O_2$, $H_2$, and ratios of CO to $CO_2$ measured close to the ground at the Battersby fire are shown in Figure 28.11). This correlation between CO to $CO_2$ ratios and $CH_4$ emissions is illustrated by a linear regression of the $CH_4$ emission factor onto the

**Table 28.4** Average emission factors (and standard deviations) for various trace gases from 10 biomass fires in North America

| Fire | CO | $CO_2$ | $O_3$ | $NH_3$ | $CH_4$ | $C_3H_6$ | $C_2H_6$ | $C_3H_8$ | $C_2H_2$ | N-$C_4$[a] | $N_2O$ | F12[b] | $NO_x$[c] |
|---|---|---|---|---|---|---|---|---|---|---|---|---|---|
| Lodi 1 | 74 ± 16 | 1664 ± 44 | 14 ± 13 | 1.7 ± 0.8 | 2.4 ± 0.15 | 0.58 ± 0.05 | 0.35 ± 0.12 | 0.21 ± 0.12 | 0.32 ± 0.05 | 0.11 ± 0.07 | 0.31 ± 0.14 | 0.045 ± 0.010 | 8.9 ± 3.5 |
| Lodi 2 | 75 ± 14 | 1650 ± 31 | 0.19 ± 0.36 | 0.09 ± 0.04 | 3.6 ± 0.25 | 0.46 ± 0.03 | 0.55 ± 0.15 | 0.32 ± 0.12 | 0.21 ± 0.03 | 0.10 ± 0.05 | 0.27 ± 0.31 | 0.009 ± 0.003 | 3.3 ± 0.8 |
| Myrtle Fall Creek | 106 ± 20 | 1626 ± 39 | −0.5 ± 0.2 | 2.0 ± 0.9 | 3.0 ± 0.8 | 0.7 ± 0.04 | 0.60 ± 0.13 | 0.25 ± 0.05 | 0.22 ± 0.04 | 0.02 ± 0.04 | — | 0.0025 ± 0.0015 | 2.54 ± 0.70 |
| Silver | 89 ± 50 | 1637 ± 103 | 4.7 ± 4.0 | 0.6 ± 0.5 | 2.6 ± 1.6 | 0.08 ± 0.01 | 0.56 ± 0.33 | 0.42 ± 0.13 | 0.19 ± 0.09 | 0.2 ± 0.1 | 0.27 ± 0.39 | 0.0 | 0.81 ± 0.69 |
| Hardiman | 82 ± 36 | 1664 ± 62 | −0.5 ± 0.4 | 0.1 ± 0.07 | 1.9 ± 0.5 | 0.58 ± 0.09 | 0.45 ± 0.26 | 0.18 ± 0.13 | 0.31 ± 0.35 | 0.02 ± 0.04 | 0.41 ± 0.52 | 0.0004 ± 0.0003 | 3.3 ± 2.3 |
| Eagle | 34 ± 6 | 1748 ± 11 | 6.5 ± 2.9 | — | 0.9 ± 0.2 | 0.25 ± 0.06 | 0.18 ± 0.05 | 0.05 ± 0.02 | 0.08 ± 0.02 | 0.2 ± 0.08 | 0.16 ± 0.013 | 0.008 ± 0.003 | 7.2 ± 3.8 |
| Battersby | 175 ± 91 | 1508 ± 161 | −0.9 ± 0.6 | — | 5.6 ± 1.7 | 0.9 ± 0.15 | 0.57 ± 0.45 | 0.27 ± 0.12 | 0.33 ± 0.06 | 0.07 ± 0.06 | — | — | 1.05 ± 1.33 |
| Hill | 90 ± 21 | 1646 ± 50 | −0.29 ± 0.12 | — | 4.2 ± 1.3 | 0.65 ± 0.19 | 0.48 ± 0.17 | 0.15 ± 0.06 | 0.25 ± 0.05 | 0.04 ± 0.01 | 0.18 ± 0.06 | 0.0 | — |
| Wicksteed | 55 ± 41 | 1700 ± 82 | −1.25 ± 1.16 | — | 3.8 ± 2.8 | 0.62 ± 0.40 | 0.51 ± 0.34 | 0.17 ± 0.12 | 0.22 ± 0.12 | 0.04 ± 0.03 | 0.22 ± 0.14 | 0.0017 ± 0.0022 | — |
| Mabel Lake | 83 ± 37 | 1660 ± 70 | −0.3 ± 0.4 | — | 3.5 ± 1.9 | 0.46 ± 0.21 | 0.38 ± 0.21 | 0.11 ± 0.07 | 0.22 ± 0.06 | 0.03 ± 0.01 | 0.04 ± 0.05 | 0.0 | — |
| Overall average emission factor | 83 ± 16 | 1650 ± 29 | 2.2 ± 1.6 | 0.90 ± 0.43 | 3.2 ± 0.5 | 0.53 ± 0.08 | 0.46 ± 0.08 | 0.21 ± 0.05 | 0.24 ± 0.04 | 0.083 ± 0.028 | 0.23 ± 0.05 | 0.0074 ± 0.0051 | 3.9 ± 16 |

Note: With the exception of $O_3$ and $NH_3$, for which values are based on continuous measurements and filters, respectively, all values shown are based on the analyses of samples collected in steel canisters. Units are g $kg^{-1}$. From Hegg et al. (1990).

a. Straight chain paraffin with carbon number of 4.

b. $CF_2Cl_2$

c. $NO_x = NO + NO_2$

**Table 28.5** Mean values of $EF_x/EF_{CO}$ for biomass burning (where $EF_x$ is the emission factor of trace gas species $x$ and $EF_{CO}$ the emission factor of CO) calculated from the data listed in Table 28.4[a]

| Species | $EF_x/EF_{CO}$ | Estimated flux from biomass burning worldwide (Tg $yr^{-1}$) | Estimated contribution of biomass burning to worldwide flux of species (%) |
|---|---|---|---|
| $O_3$ | 0.04 ± 0.03 | 32 | 1 |
| $NH_3$ | 0.01 ± 0.008 | 8 | 50 |
| $CH_4$ | 0.04 ± 0.008 | 32 | ~7 |
| $C_3H_6$ | 0.007 ± 0.001 | 6 | ? |
| $C_2H_6$ | 0.006 ± 0.001 | 5 | ? |
| $C_3H_8$ | 0.003 ± 0.0007 | 2.4 | ? |
| $C_2H_2$ | 0.003 ± 0.0006 | 2.4 | ? |
| $N\text{-}C_4$ | 0.001 ± 0.0007 | 0.8 | ? |
| $N_2O$ | 0.003 ± 0.001 | 2.4 | 16 |
| $F_{12}$ | 0.0001 ± 0.00007 | 0.08 | 20 |
| | (0.00005 ± 0.00003)[b] | (0.04)[b] | (10)[b] |
| $NO_x$ | 0.07 ± 0.04 | 56 | 40 |

Note: Also shown are estimates of the global fluxes of various trace gases from biomass burning based on the $EF_x/EF_{CO}$ ratios and estimates of worldwide CO emissions from biomass burning from Crutzen et al. (1985). From Hegg et al. (1990).
a. The mean values of $EF_x/EF_{CO}$ were obtained by first ratioing the values of $EF_x$ to $EF_{CO}$ for each of the fires listed in Table 28.4 and then averaging these 10 ratios.
b. A more conservative estimate obtained by eliminating results from the Lodi 1 fire.

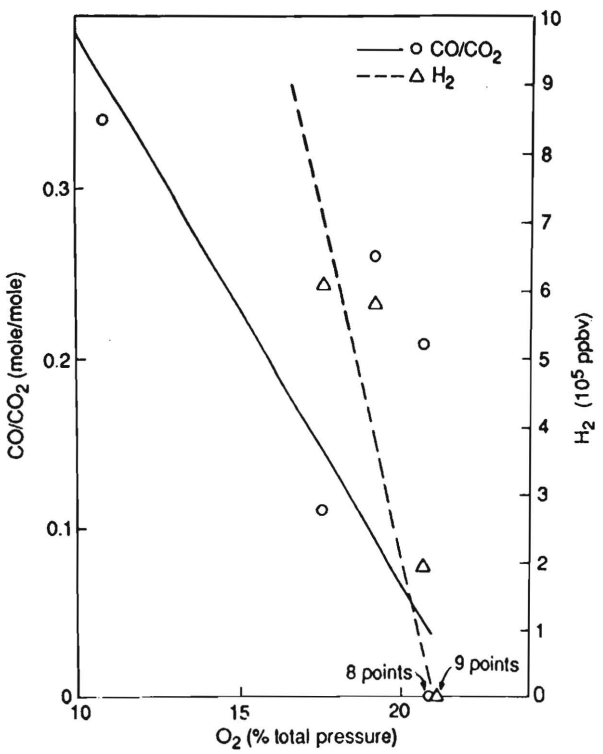


**Figure 28.11** Concentration ratio of $CO/CO_2$ (circles) and $H_2$ concentration (triangles) versus $O_2$ in the plume from the Battersby fire. The data were obtained at or within 100 m of the ground. The lines shown are linear regressions (from Hegg et al., 1990).

ratio of CO to $CO_2$ emission factors using the data in Table 28.4. Such a calculation yields a correlation coefficient ($r$) of 0.75 significant at >98% confidence level, thus suggesting that biomass fires are often oxygen limited. A graphical presentation of this regression analysis is given in Figure 28.12.

Based on the data listed in Table 28.5, we obtain an estimated global flux of nonmethane hydrocarbons (NMHC) from fire emissions of about 15 Tg $yr^{-1}$. In view of the fact that only a portion of all the NMHCs have been incorporated into our data set, together with the uncertainties in the calculations, this value is in reasonable agreement with the result of about 30 Tg $yr^{-1}$ obtained by Crutzen et al. (1985).

Measurements of $N_2O$ emissions from combustion sources have recently come under scrutiny due to the discovery of an artifact in the use of sampling containers. Muzio and Kramlich (1988) have found that the storage of moist combustion products containing $SO_2$ and NO for relatively short periods can stimulate the production of high concentrations (on the order of several hundred parts per million, ppm) of $N_2O$ in containers that previously contained no $N_2O$. Many of our trace gas measurements are based on steel canister samples. We do not, however, feel our $N_2O$ measurements are artifacts. The concentrations of $SO_2$ required for $N_2O$ formation in the containers are at least three orders of magnitude larger than the $SO_2$ concentrations we measured in the plumes from the fires in this study (Muzio and Kramlich stated that

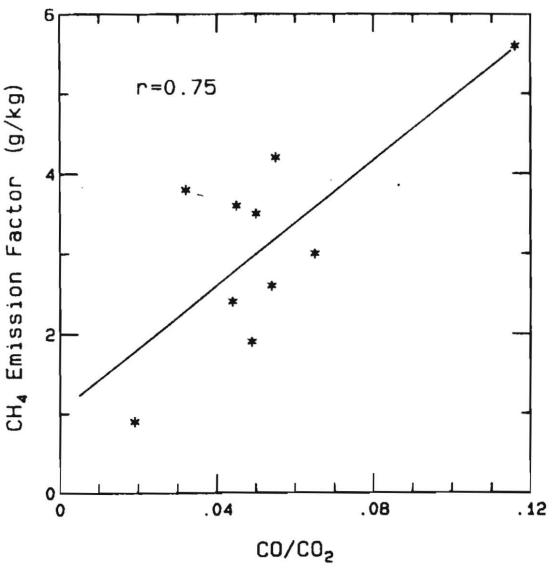


**Figure 28.12** $CH_4$ emission factor versus the ratio of CO to $CO_2$ emission factors for ten of the seventeen fires studied. r is the correlation coefficient, and the line shown is a linear regression. Data is taken from Table 28.4.

$SO_2$ concentrations below 600 ppm resulted in negligible production of $N_2O$; typical $SO_2$ concentrations we have measured are only on the order of 1 to 15 ppb).

The estimated global flux of $N_2O$ shown in Table 28.5 (2.4 Tg $yr^{-1}$) corresponds to an emission of about 1.5 Tg N $yr^{-1}$. This value is essentially the same as the estimate of 1.6 Tg N $yr^{-1}$ by Crutzen et al. (1985). Our emission flux of 2.4 Tg $N_2O$ $yr^{-1}$ represents approximately 16% of the total worldwide flux of the species, thereby strengthening the contention that biomass burning contributes significantly to the atmospheric $N_2O$ reservoir.

One persistent, unexpected, and not completely explained feature of our biomass fires is the presence of freons in the smoke. Because F12 cannot be produced by fires, the presence of this trace gas in the smoke plume must be due to the resuspension of F12 that had been previously deposited onto the fuel bed (Hegg et al., 1990).

Our estimated flux of F12 from biomass burning (0.08 Tg $yr^{-1}$) represents a significant fraction (about 20%) of the annual global emission of this species (this percentage value was calculated using the National Research Council (1983) emission estimate of 0.4 Tg $yr^{-1}$ of F12). This suggests that the deposition of F12 may be significant globally. This hypothesis is contrary to the current belief that the only sink for F12 that is important in atmospheric budget calculations is loss by photodisassociation in the stratosphere. While the actual method by which freons could be sequestered in biomass or soils is uncertain, we are confident that this result is not an artifact. We do, however, have some concern about the results from Lodi 1, which may be anomalous (see Table 28.4). These elevated emissions heavily influenced the average value of the F12/CO ratio used in calculating the flux of F12 due to biomass burning (for a detailed discussion of our concerns with the F12 emissions from the Lodi 1 fire, the reader is referred to the paper by Hegg et al., 1990). However, a calculation of the global flux of F12 that omits the Lodi 1 fire emission measurements yields a value of 0.04 Tg $yr^{-1}$. This result is still a significant fraction (about 10%) of the total global flux of F12, thus suggesting that surface deposition may indeed be an important sink for tropospheric F12.

Our estimated flux of $NO_x$ from fire emissions is 56 Tg $yr^{-1}$ (Table 28.5). This value corresponds to about 19 Tg N $yr^{-1}$ (Hegg et al., 1990). By comparison, a previous estimate of the global flux of $NO_x$ due to biomass burning yielded a value of 12 Tg N $yr^{-1}$ with a range of 4 to 24 Tg N $yr^{-1}$ (Logan, 1983). Even though our estimate of 19 Tg N $yr^{-1}$ falls within Logan's wide range, our emission value suggests that the flux of $NO_x$ from fire emissions may be more important than has been assumed previously. Further evidence for the impact of biomass burning on the worldwide flux of $NO_x$ arises from the fact that our estimated flux value is about 40% of total $NO_x$ emissions. This indicates that $NO_x$ emissions from fires are comparable to emissions of this species from fossil fuel combustion (c.f. Crutzen et al., 1979; Logan, 1983).

A fraction of the high emission of $NO_x$ from biomass burning is evidently due to the revolatilization of $NO_x$ that had been previously deposited on the fuel bed (for further discussion of this process, the reader is referred to Hegg et al., 1988, 1990.) It appears therefore that resuspension by biomass burning of previously deposited urban/industrial $NO_x$ should be included in global flux estimates.

## Summary and Conclusions

Our field studies of biomass burning indicate that rather different amounts of particles and trace gases are produced as a result of a complex interplay between fuel types (including surface and soil organics), fuel conditions (primarily moisture content), and combustion physics (meteorology, spatial distribution of the fuels, and the scale and character of the fire). In

view of the variances generated by these poorly defined interactions, we hesitate to extrapolate our measurements and observations beyond the temperate zone in which they were obtained. Nevertheless, with respect to global change implications, the main features of our work may be summarized as follows:

- The particle emission factor (for particles <3.5 μm diameter) for all of the fires studied averaged 15 grams per kilogram of fuel burned.
- Biomass smoke particles have a size distribution characterized by prominent nucleation (<0.1 μm), accumulation (0.1 to 2 μm) and coarse (>2 μm) modes. The accumulation mode generally dominates smoke mass and visible light optical properties.
- The single scattering albedo of the smokes at visible wavelengths averaged 0.83 ± 0.11 and the specific absorption averaged 0.64 ± 0.36 $m^2\ g^{-1}$.
- A large fraction (30% to 100%) by mass of the smoke particles produced in biomass burning are efficient cloud condensation nuclei (CCN).
- Estimates of the global production of CCN by biomass burning suggest a flux of about $10^{19}$ to $10^{22}$ CCN $s^{-1}$. This is similar to other globally important sources of CCN.
- Large biomass fires are often capped by cumulus clouds. When the cloud depth exceeds 2 km, a large fraction of the smoke particles are scavenged by the capping cloud.
- Biomass burning may account for as much as 50% of global emissions of $NH_3$.
- The combination of $NH_3$ and $NH_4^+$ emissions from biomass burning may dominate the global $NH_3$ cycle.
- Pollutants such as $NO_x$ and $SO_2$, which have been previously deposited on biomass fuels, may be volatilized and resuspended in the atmosphere by biomass burning. This effect is likely most important in urban regions.
- Resuspension of F12 during biomass burning suggests that surface deposition may be an important, and previously unrecognized, sink for F12.
- As fires increase in size, the combustion process may become oxygen deficient causing a more prolific production of smoke particles and saturated hydrocarbons (such as $CH_4$) than might otherwise be expected.

**Acknowledgments**

This contribution summarizes the results from a long period of research on biomass fires that would not have been possible without the able assistance of the technical, scientific, and aviation staff of University of Washington's Cloud and Aerosol Research Group. The work was supported by the following grants and contracts: Naval Research Laboratory Contract No. N0014-86-C-2246, Sandia National Laboratories Contract No. 57-0343, U.S. Department of Agriculture Forest Service cooperative agreement No. PSW-87-0020, Defense Nuclear Agency under Project IACRO 89-903, Task RA, Work Unit 00024, British Columbia Ministry of Forestry, and Intermountain Research Station, Forest Service, U.S. Department of Agriculture Agreement No. INT-89426-RJVA. We thank all of these organizations for their support.

## REFERENCES


Andreae, M. O., E. V. Browell, M. Garstang, G. L. Gregory, R. C. Harriss, G. L. Hill, D. J. Jacob, M. C. Pereira, G. W. Sachse, A. W. Setzer, P. L. Silva Dias, R. W. Talbot, A. L. Torres and S. C. Wofsy, 1988: Biomass burning emissions and associated haze layers over Amazonia. *J. Geophys. Res.*, *93*, 1509-1527.

Bryam, G. M., 1959: Combustion of Forest Fuel. *In Forest Fire Control and Use*, K. P. Davis (ed.), McGraw-Hill, New York, NY, 321 pp.

Cofer III, W. R., J. S. Levine, D. I. Sebacher, E. L. Winstead, P. J. Riggan, J. A. Brass, and V. G. Ambrosia, 1988: Particulate emissions from a mid-latitude prescribed chaparral fire. *J. Geophys. Res.*, *93*, 5207-5212.

Cofer III, W. R., J. S. Levine, D. I. Sebacher, E. L. Winstead, P. J. Riggan, B. J. Stocks, J. A. Brass, V. G. Ambrosia, and P. J. Boston, 1989: Trace gas emissions from chaparral and boreal forest fires. *J. Geophys. Res. 94.*, 2255-2259.

Cotton, W. R., 1985: Atmospheric convection and nuclear winter. *Amer. Sci.*, *73*, 275-280.

Crutzen, P. J., L. E. Heidt, J. P. Krasnec, W. H. Pollock, and W. Seiler, 1979: Biomass burning as a source of the atmospheric gases CO, $H_2$, $N_2O$, NO, $CH_3Cl$ and COS, *Nature*, *282*, 253-256.

Crutzen, P. J., A. C. Delany, J. Greenberg, P. Haagenson, L. Heidt, R. Lueb, W. Pollock, W. Seiler, A. Wartburg and P. Zimmerman, 1985: Tropospheric chemical composition measurements in Brazil during the dry season. *J. Atmos.Chem.*, *2*, 233-256.

Dismitriodes, B., and M. Dodge (Eds), 1983: *Proceedings of the Empirical Kinetic Modeling Approach (EKMA) Validation Workshop*, EPA Report No. 60019-83-014, August, 1983.

Eagan, R. C., P. V. Hobbs, and L. F.Radke, 1974: Particle emissions from a large kraft paper mill and their effects on the microstructure of warm clouds. *J.Appl. Meteor.*, *13*, 535-552.

Einfeld, W., B. Mokler, D. Morrison, and B. Zak, 1989: Particle and trace element production from fires in the chaparral fuel type. *Twenty-Fifty Session of the Air and Waste Management Association* (Available from D. E. Ward, USDA Forest Service, Intermountain Fire Science Laboratory, Missoula, MT 59807).

Evans, L. F., M. K. King, P. R. Pockhaun, and L.T.Stephens,1974: Ozone measurements in smoke from forest fires. *Environ. Sci. Technol.*, *8*, 75-79.

Fuchs, N. A., 1964: *The Mechanics of Aerosols*. Pergamon Press, New York.

Galbally, L. E., 1985: The emission of nitrogen to the remote atmosphere: background paper. In *Biogeochemical Cycling of Sulphur and Nitrogen in the Remote Atmosphere*, edited by J. H. Galloway, R. J. Charlson, M. O. Andreae, and H. Rodhe, pp. 27-53, D. Reidel Pub., Heigham, MA.

Hallett, J., J. Hudson and C. F. Rogers, 1989: Characterization of combustion aerosols for haze and cloud formation. *Aerosol Science & Technology*, *10*, 70-83.

Hegg, D. A., L. F. Radke, P. V. Hobbs, C. A. Brock, and P. J. Riggan, 1987; Nitrogen and sulfur emissions from the burning of forest products near large urban areas. *J. Geophys. Res.*, *92*, 14701-14709.

Hegg, D. A., P. V. Hobbs, and L. F. Radke, 1984: Measurements of the scavenging of sulfate and nitrate in clouds. *Atmos. Environ.*, *18*, 1939-1946.

Hegg, D. A., L. F. Radke, P. V. Hobbs, and P. J. Riggan, 1988: Ammonia emissions from biomass burning, *Geophys. Res. Lett.*, *1*, 335-337.

Hegg, D. A., L. F. Radke, P. V. Hobbs, R. A. Rasmussen, and P. J. Riggan, 1990: Emissions of some trace gases from biomass fires. *J. Geophys. Res.*, *95*, 5669-5675.

Hobbs, P. V., and L. F. Radke, 1969: Cloud condensation nuclei from a simulated forest fire. *Science*, *163*, 279-280.

Jaenicke, R., 1981: in *Climatic Variations and Variability: Facts and Theories*, edited by A. Berger, Reidel, Dordrecht, 577-597.

Jensen, J. B., and R. J. Charlson, 1984: On the efficiency of nucleation scavenging. *Tellus*, *36B*, 367-375.

Logan, J.A., Nitrogen oxides in the troposhpere: global and regional budgets, 1983: *J. Geophys. Res.*, *88*, 10,785-10807.

McMahon, C. K., 1983: Characteristics of forest fuels, fires and emissions. Paper 83-45.1, presented at the *76th Annual Meeting of the Air Pollution Control Association*, Atlanta, GA, 19-24 June.

Mooney, H. A., P. M. Vitousek, and P. A. Watson, 1987: Exchange of materials between terrestial ecosystems and the atmosphere, *Science*, *238*, 926-932.

Muzio, L. J., and J. C. Kramlich, 1988: An artifact in the measurement of $N_2O$ from combustion sources, *Geophys. Res. Lett.*, *15*, 1369-1372.

National Academy of Sciences, 1984: *Global Tropospheric Chemistry: A Plan for Action*. National Academy Press, Washington, DC, 194 pp.

National Academy of Sciences, 1986: *Global Tropospheric Chemistry: Plans for the U.S. Research Effort*. National Academy Press, Washington, DC, 110 pp.

National Research Council, 1983: *Causes and Effects of Changes in Stratospheric Ozone: Update*, National Academy Press, Washington, D.C.

Patterson, E. M. and C. K. McMahon, 1984: Absorption characteristics of forest fire particulate matter. *Atmos. Environ.*, *18*, 11,2541-11,2551.

Radke, L. F., 1983: Preliminary measurements of the size distribution of cloud interstitial aerosol. In *Precipitation Scavenging, Dry Deposition and Resuspension*, H. R. Pruppacher, R. G. Semonin, and W. G. N. Slinn (eds.), Elsevier, New York, NY, 71-78.

Radke, L.F., 1989: Airborne observations of cloud microphysics modifed by anthropogenic forcing, in *Proceedings of a Symposium on the Role of Clouds in Atmospheric Chemistry and Global Climate*, American Meteorological Society, pp. 310-315, Anaheim, California, 29 January - 3 February.

Radke, L. F., and P. V. Hobbs, 1976: Cloud condensation nuclei on the Atlantic seaboard of the United States. *Science*, *193*, 999-1002.

Radke, L. F., J. L. Stith, D. A. Hegg, and P. V. Hobbs, 1978: Airborne studies of particles and gases from forest fires. *J. Air Pollut. Control Assoc.*, *28*, 30-34.

Radke, L. F., D. A. Hegg, J. H. Lyons, C. A. Brock, and P. V. Hobbs, 1988: Airborne measurements on smokes from biomass burning. In *Aerosols and Climate*, P. V. Hobbs and M. P. McCormick (eds.), pp. 411-422, A. Deepak Publishing Co., Hampton, VA.

Radke, L. F., A. S. Ackerman, D. A. Hegg, J. H. Lyons, P. V. Hobbs, and J. E. Penner, 1990a: Effects of aging on the smoke from a forest fire: Implications for the nuclear winter hypothesis. *J. Geophys. Res.* (in press).

Radke, L. F., J. H. Lyons, P. V. Hobbs, and R. E. Weiss, 1990b: Smokes from the burning of aviation fuels and their self-lofting by solar heating. *J. Geophys. Res.* (in press).

Radke, L. F., J. H. Lyons, P. V. Hobbs, D. A. Hegg, D. V. Sandberg, and D. E. Ward, 1990: Airborne monitoring and smoke characterization of prescribed fires on forest lands in western Washington and Oregon. *Final Report, USDA Forest Service, General Technical Report PNW-GTR-251*, 81 pp.

Seiler, W., and P. V. Crutzen, 1980: Estimates of gross and net fluxes of carbon between the biosphere and the atmosphere from biomass burning. *Climatic Change*, *2*, 207-248.

Stith, J. L., L. F. Radke, and P. V. Hobbs, 1981: Particle emissions and the production of ozone and nitrogen oxides from the burning of forest slash. *Atmos. Environ.*, *15*, 73-82.

Susott, R. A., D. E. Ward, R. E. Babbitt, and D. J. Latham, 1990: The measurement of trace emissions and combusion characteristics for a mass-fire. (This proceedings).

Twomey, S., and T. A. Wojciechowski, 1969: Observations of the geographical variation of cloud nuclei. *J. Atmos. Sci.*, *26*, 684-688.

Waggoner, A. P., R. E. Weiss, N. C. Ahlquist, D. S. Covert, S. Will, and R. J. Charlson, 1981: Optical characteristics of atmospheric aerosols. *Atmos. Environ.*, *15*, 1891-1909.

Ward, D. E., D. V. Sandberg, R. D. Ottman, J. A. Anderson, G. G. Hofner, and C. K. Fitzsimmons, 1982: Measurements of smokes from two prescribed fires in the Pacific Northwest. *Seventy-Fifth Annual Meeting of the Air Pollution Control Association* (Available from D. E. Ward, USDA Forest Service, Intermountain Fire Science Laboratory, Missoula, MT 59807).

Ward, D. E., and Hardy, C. C., 1990: Smoke emissions from wildland fires. *Environment International*, *17*, 117-134.

Ward, D. E., 1990: Factors influencing the emissions of gases and particulate matter from biomass burning. *In Fire in the Tropical Biota*, J. G. Goldammer (ed.), Springer-Berlag, Heidelber (in press).

Warner, J., and S. Twomey, 1967: The production of cloud nuclei by cane fires and the effect on cloud droplet concentration. *J. Atmos. Sci.*, *24*, 704.

Weiss, R. E., and L. F. Radke, 1990: Optical extinction and absorption of smokes from large fires: absorption techniques and observations. *J. Atmos. Ocean. Tech.*